Principles of nuclear magnetic ordering

M. Goldman, M. Chapellier*, Vu Hoang Chau, and A. Abragam
Service de Physique du Solide et de Résonance Magnétique, Centre d'Etudes Nucléaires de Saclay, B.P. 2-91190-Gif-sur-Yvette, France
(Received 12 June 1973)

We describe in this article the principles of production and observation of magnetic ordering in systems of nuclear spins subjected to dipole-dipole interactions. The cooling necessary for producing ordering, which concerns only the nuclei, is obtained by a two-step process: dynamic polarization in a high field followed by adiabatic nuclear demagnetization. The study is mostly limited to adiabatic demagnetization in the rotating frame, for which the effective nuclear spin-spin interactions are truncated dipolar interactions. We list briefly a number of measurements that can be made, mostly relevant to magnetic resonance techniques, together with the information they yield on the ordering. The prediction of the nature of ordered structures, both at positive and negative temperatures, is made through the use of the local Weiss-field approximation. In the case of simple cubic systems of spins 1/2, one predicts the occurrence of three different antiferromagnetic structures. The Weiss-field approximation, occasionally supplemented with high-temperature approximation to spin temperature theory, is finally used for predicting as a function of entropy various properties of the antiferromagnetic states: sublattice magnetizations, transition entropy, transverse and longitudinal susceptibilities, transition field, and shape of the fast-passage dispersion signal.

I. INTRODUCTION

Following the early proposal of a method for producing magnetic ordering in systems of nuclear spins subjected to dipole-dipole interactions,[1,2] experiments have been performed in calcium fluoride and lithium fluoride that provided evidence for the existence of antiferromagnetism, in CaF_2 and LiF,[3-10] and of ferromagnetism, in CaF_2.[9-11] In the short publications describing these results we contented ourselves with a brief description of the techniques of production and observation of nuclear magnetic ordering and of the theoretical methods used for describing the nature and properties of the ordered states.

The purpose of the present article is to give a fuller description of some of the principles and methods used in this study.

In the rest of the Introduction we recall briefly the nature of the problem investigated and the principle of production of nuclear magnetic ordering, and we give a short list of the types of measurements that can be made.

This is followed, in Sec. II, by the description of the local Weiss-field approximation, as applied to simple cubic systems of spins $\frac{1}{2}$ subjected to truncated dipole-dipole interactions, for predicting the ordered structures occurring at low temperature. Finally, Sec. III uses a combination of Weiss-field and high-temperature approximations for predicting the properties of antiferromagnetic structures as a function of field and temperature. This last part is limited to the analysis of a particular antiferromagnetic structure, observed in calcium fluoride, on which most of the measurements have been performed so far. Some of the published experimental results are reproduced on the figures, for the purpose of testing the validity of the theoretical curves.

Use of more sophisticated theoretical methods and investigation of other structures are deferred to future publications. One may note, however, that a detailed analysis of nuclear antiferromagnetism by the spin-wave and the random-phase approximations has been given in a thesis (Ref. 7) to which the reader is referred.

A. Summary of the principle of production of nuclear magnetic ordering

The production of magnetic ordering in nuclear spin systems subjected to dipole-dipole interactions requires exceedingly low temperatures, as a consequence of the smallness of these interactions. As a rough estimate, the critical temperature T_c for these systems is such that $k_B T_c$ is comparable with the interaction energy between nuclei nearest neighbors. The latter being typically of the order of a few kHz (in frequency units), the temperature T_c is expected to be of the order of 10^{-6} K or less, which is well outside the reach of present cryogenic techniques.

We use a cooling process in which only the nuclear spins are cooled to the microdegree range, whereas the lattice remains at relatively high temperature (typically 0.3 K in our experiments). An obviously necessary condition is that one can find nuclear spin systems sufficiently loosely coupled to the lattice to be practically isolated during a time T_1 long enough to perform observations on them. Furthermore, it is necessary that these isolated systems reach in a time T_2 much shorter than T_1 a state of internal equilibrium character-

ized by a temperature. The first condition can be fulfilled by using an insulating diamagnetic solid at low temperature. As for the second one, its validity has been postulated long ago and used as the basis of the spin-temperature theory. This theory has been verified in a great many experiments[12] but, apart from the present work, only under high-temperature conditions, that is, when $k_B T$ is much larger than the average energy per spin. It is only under very special conditions but this theory has been observed to fail.[13] The present study is based on the assumption that the spin-temperature concept remains valid even at low temperature. It is justified by the experimental results obtained so far.

The nuclear cooling process used in this study is a two-step process which works as follows.

(a) The nuclear spins are dynamically polarized in a high external field H_0 by the solid effect,[14] i.e., by inducing with a microwave field of appropriate frequency flip-flop transitions between the nuclear spins and suitable electronic spins present at low concentration in the sample. Increasing the polarization of the nuclear spins is equivalent to a cooling, as shown for instance for spins $\frac{1}{2}$. Their polarization P is related to their temperature T according to

$$P = \tanh(\hbar\omega_0/2k_B T) , \tag{1}$$

so that, say, in a field where $\omega_0/2\pi = 100$ MHz, a polarization of 50% corresponds to a spin temperature $T \simeq 4.7\times10^{-3}$ K.

(b) The polarized nuclear spins are subjected to an adiabatic demagnetization, which at the same time reduces their Hamiltonian to its dipolar part and decreases their temperature by a large factor. The cooling achieved by this step is limited by the residual dipolar field at the nuclear site—Weiss-field when the final state is magnetically ordered, or local field when it is not. An order-of-magnitude calculation within the high-temperature approximation to spin-temperature theory[5] yields a decrease of temperature by a factor approximately 10^4 from a field of say 25 kG to zero applied field, which together with the cooling achieved in the first step, is sufficient to bring the spin temperature into the microdegree range necessary for the production of ordering.

It is in fact simpler to discuss this process in terms of entropy rather than temperature: The dynamic polarization of the nuclear spins in high field decreases their entropy, and the adiabatic demagnetization simply removes the unwanted high field while keeping the entropy constant.

One consequence of the fact that we are dealing with nuclear spin systems isolated from the lattice is that we can study their low-temperature properties not only when their interactions are the ordinary dipole-dipole interactions, but also when they are truncated dipole-dipole interactions. This is done by performing the adiabatic demagnetization either in the laboratory frame or in the rotating frame, respectively. These notions are very familiar in nuclear magnetism. We recall them very briefly.

Following an adiabatic demagnetization in the laboratory frame, that is, an actual decrease of the applied field to zero, the final Hamiltonian of the system reduces to its dipole-dipole Hamiltonian. If we suppose that the sample contains only one nuclear species of spins I, this Hamiltonian is of the form

$$\mathcal{H}_D = \frac{1}{2}\sum_{i,j}\frac{\gamma^2\hbar}{r_{ij}^3}\left(\vec{I}_i\cdot\vec{I}_j - 3\,\frac{(\vec{I}_i\cdot\vec{r}_{ij})(\vec{I}_j\cdot\vec{r}_{ij})}{r_{ij}^2}\right) , \tag{2}$$

where r_{ij} is the distance between spins i and j.

That the demagnetization ends up with a cooling of $\mathcal{H}_D$ results from the fact (well established in the high-temperature limit) that a fast thermal mixing between Zeeman and dipolar interactions takes place as soon as the applied field becomes less than a few times the local dipolar field. The mixing time decreases steeply with applied field and reaches eventually a value T_2 typically of the order of 100 μsec. The total Hamiltonian being

$$\mathcal{H} = -\gamma H_0 I_z + \mathcal{H}_D = \omega_0 I_z + \mathcal{H}_D ,$$

thermal equilibrium corresponds to a density matrix of the form

$$\sigma = e^{-\beta\mathcal{H}}/\mathrm{Tr}(e^{-\beta\mathcal{H}}) , \tag{3}$$

where β is the inverse temperature.

In a high field, on the other hand, that is, when the Zeeman interaction is much larger than the dipole-dipole one, the establishment of a thermal equilibrium within the spin system is exceedingly slow. It can be shown that the system possesses two quasiconstants of the motion: the Zeeman interaction $\omega_0 I_z$ and the secular part $\mathcal{H}'_D$ of the dipole-dipole interaction, that is, that part of $\mathcal{H}_D$ which commutes with I_z. This so-called secular or truncated dipole-dipole interaction is of the form

$$\mathcal{H}'_D = \frac{1}{2}\sum_{i,j} A_{ij}(2I_z^i I_z^j - I_x^i I_x^j - I_y^i I_y^j) , \tag{4}$$

with

$$A_{ij} = \tfrac{1}{2}\gamma^2\hbar\,(1 - 3\cos^2\theta_{ij})\,r_{ij}^{-3} , \tag{5}$$

where θ_{ij} is the angle between the applied field $\vec{H}_0$ and $\vec{r}_{ij}$.

One can establish a thermal contact between Zeeman and truncated dipolar interactions by irradiating the sample with an rf field H_1 perpendicular to $\vec{H}_0$ and rotating with a frequency ω close to the Larmor frequency $\omega_0 = -\gamma H_0$ of the spins. In a frame rotating with frequency ω, the evolution of

the density matrix of the spin system depends on the following effective Hamiltonian:

$$\mathcal{H}^* = \Delta I_z + \omega_1 I_x + \mathcal{H}'_D \ . \tag{6}$$

The spin-temperature theory states that the system evolves toward a state of equilibrium characterized by a temperature in the rotating frame, i.e., that its density matrix in the rotating frame becomes

$$\sigma = e^{-\beta\mathcal{H}^*}/\mathrm{Tr}\{\cdots\} \ . \tag{7}$$

The rate of achievement of equilibrium, which we can formally calculate as a function of Δ and ω_1,[12] can be made fast. The so-called adiabatic demagnetization in the rotating frame is performed by a fast passage[15]: One applies an rf field at a distance Δ from resonance such that $|\Delta| \gg |\mathcal{H}'_D|$ and slowly decreases $|\Delta|$ to zero. The final Hamiltonian is $\omega_1 I_x + \mathcal{H}'_D \simeq \mathcal{H}'_D$ if ω_1 is small. One can also decrease adiabatically ω_1 to zero, so that the Hamiltonian is truly $\mathcal{H}'_D$.

Once we have made $\omega_1 = 0$, there is no need of using a rotating frame any more and we can consider the system as viewed from the laboratory frame. Since in a high field there are two quasiconstants of the motion, $\omega_0 I_z$ and $\mathcal{H}'_D$, the quasiequilibrium form of the density matrix is

$$\sigma = e^{-\alpha\omega_0 I_z - \beta\mathcal{H}'_D}/\mathrm{Tr}\{\cdots\} \ , \tag{8}$$

with two different inverse temperatures α and β for the two quasiconstants of the motion. The effect of the fast passage is to make $\alpha = 0$ and β large.

All experiments performed so far have used adiabatic demagnetization in the rotating frame, and the rest of this paper is restricted to the study of the low-temperature properties of the truncated Hamiltonian $\mathcal{H}'_D$.

The main characteristics of this study are the following.

(a) The Hamiltonian $\mathcal{H}'_D$ is known with certainty, with no adjustable parameter. The study of nuclear dipolar magnetic ordering is then a "clean" problem that affords a test of the validity of the approximate statistical theories of magnetism. The situation is not quite so bright because of the presence of the electronic paramagnetic impurities necessary for performing the dynamic polarization. Their perturbating influence can be rendered negligible by decreasing their concentration. It is up to experiment to determine which concentrations are acceptable.

(b) The Hamiltonian $\mathcal{H}'_D$ depends on the orientation of the external field H_0 through the values of θ_{ij} [Eqs. (4) and (5)], so that the ordered structures are likely to depend on this orientation.

(c) The spin temperature in the demagnetized state can be made at will positive or negative, depending on the sign of $\Delta = \omega_0 - \omega$ when starting the fast passage. This possibility, well known in nuclear magnetism, is linked to the fact that the dipolar Hamiltonian has an upper bound to its energy spectrum. When $T \to +0$, the state of the system is that of lowest energy; when $T \to -0$, it is that of highest energy. It is then possible, with the same Hamiltonian $\mathcal{H}'_D$, to study two different orderings.

(d) It is not the temperature which is the most directly accessible parameter, but the entropy of the system.

B. Types of measurements

We list briefly some of the measurements that can be performed and the kind of information they yield. Most use the techniques of magnetic resonance.

1. Dispersion signal during the fast passage

The dispersion signal u, which is the magnetization in phase with the rf field, is static when viewed from the rotating frame and proportional to the transverse susceptibility $\chi_\perp$ of the system. Of particular interest is the value of $\chi_\perp$ in zero effective field, that is, at the center of the fast passage. Furthermore, it suffers a noticeable change at the transition from the high-effective-field paramagnetic phase to the low-effective-field ordered phase, which offers the possibility of measuring the critical field of transition.

2. Longitudinal magnetization

The bulk longitudinal magnetization in the presence of a nonzero longitudinal effective field is proportional to the longitudinal susceptibility $\chi_\parallel$ of the system. It can be measured from the area of the absorption signal, or through the field it creates in the neighborhood of the sample, a field which can be determined for instance by the shift of the resonance frequency of liquid He^3.[6] Other schemes can be devised for measuring this susceptibility. They will be described in a different article.

3. Resonance signal in the demagnetized state

One can observe with a small nonsaturating rf field either the absorption or the dispersion signal, yielding the following information: The dispersion signal at the center of the resonance is proportional to $\chi_\perp$. The first moment of the absorption signal is proportional to the dipolar energy. This result, which will be proved elsewhere, allows a simple and accurate measurement (within a few percent) of this energy.

Let us take, for instance, the case of an antiferromagnetic structure. Recording the absorption signal at frequency ω can be shown to be equivalent to performing an antiferromagnetic resonance experiment with a field *rotating* at the low frequency $(\omega_0 - \omega)$, while benefiting from the sensitivity of

resonance at the high frequency ω. We get in that way information on sublattice magnetizations[16] as well as on spin-spin relaxation in the ordered phase.

4. Resonance of a nuclear magnetic probe

Besides the main nuclear spins whose ordering is studied, the sample may contain nuclear spins of a different species at low concentration, such as ^{43}Ca in CaF_2, ^{87}Sr in SrF_2, or ^{6}Li in LiF. Because of their low concentration, these impurity spins do not perturb the ordering of the main spins and can be used to probe this ordering on a microscopic scale, for instance when the latter create different dipolar fields at the sites of different probe nuclei, which cause a splitting of their resonance signal.[11] The impurity spins can also be used to measure the dipolar temperature T_D: When an rf field is applied at a distance Δ from their resonance, their effective Zeeman interaction ΔS_z acquires the same temperature as that of the dipolar interactions of the main spins I through thermal mixing. Their final magnetization is related in a known way [by a Brillouin function of Δ/kT_D] to this common temperature, which can thus be measured.

5. Neutron-diffraction study

Neutron diffraction, which is a unique method for ascertaining the nature of a magnetic ordered structure,[17] can be used with nuclear magnetic spins despite the very low value of their magnetic moment, because the spin-dependent part of neutron-nucleus scattering is mostly caused by strong interaction and can be much larger than their magnetic scattering.[18,19] Experimentally, this amplitude is very large for protons, which should make it easy to study the ordering of a proton system, whereas it is so small for fluorine that it is impossible to use neutron diffraction to study antiferromagnetism in calcium fluoride.

II. DERIVATION OF THE ORDERED STRUCTURES

The determination of magnetic ordered structures other than ferromagnetic is a problem that has not received a definite answer yet. One has always to resort to approximate methods open to criticism, whose validity has ultimately to be checked by experiment.

We use in this section a method developed by Villain[20] that makes use of the local Weiss-field approximation. The discussion will be limited to systems of identical spins $\frac{1}{2}$ forming a Bravais lattice with a center of symmetry and eventually specialized to the case of a simple cubic lattice. An alternative method is described in Ref. 7.

The local Weiss-field approximation is the following. When considering the interaction of a given spin $\vec{I}_i$ with all other spins of the sample, one treats only that spin $\vec{I}_i$ as a quantum-mechanical observable and replaces the spin operators of all other particles by their thermal average, i.e., by c numbers. This amounts to neglecting correlations between spins. This average interaction is equivalent to the Zeeman coupling $\vec{\omega}_i \cdot \vec{I}_i$ of the spin $\vec{I}_i$ with a fictitious magnetic field $\vec{H}_i = -\vec{\omega}_i/\gamma$, the so-called local Weiss field. We will call $\vec{\omega}_i$ the Weiss frequency.

The spin-spin energy, expressed in frequency units, takes the form

$$E = \frac{1}{2}\sum_i \vec{\omega}_i \cdot \vec{I}_i \,, \tag{9}$$

where the factor $\frac{1}{2}$ accounts for the fact that this is a self-energy.

According to Eq. (4) the components of the frequency $\vec{\omega}_i$ are

$$\begin{aligned} \omega_{ix} &= -\sum_i A_{ij}\langle I_x^j\rangle \,, \\ \omega_{iy} &= -\sum_j A_{ij}\langle I_y^j\rangle \,, \\ \omega_{iz} &= 2\sum_j A_{ij}\langle I_z^j\rangle \,. \end{aligned} \tag{10}$$

If the external field is $\vec{H}$ (this is in our case an effective field in the rotating frame) the total field experienced by the spin I_i is $\vec{H}_i^T = \vec{H} + \vec{H}_i$ and the thermal average of $\vec{I}_i$ at the inverse temperature β is given by the usual Brillouin function; that is, for a spin $\frac{1}{2}$

$$\langle \vec{I}_i \rangle = -\tfrac{1}{2}\left(\frac{\vec{\omega}_i^T}{|\vec{\omega}_i^T|}\right)\tanh\left(\tfrac{1}{2}\beta|\omega_i^T|\right) \,, \tag{11}$$

with $\vec{\omega}_i^T = -\gamma\vec{H} + \vec{\omega}_i$. We limit ourselves for the moment to the case when $\vec{H} = 0$, so that Eq. (11) becomes

$$\langle \vec{I}_i \rangle = -\tfrac{1}{2}\left(\frac{\vec{\omega}_i}{|\vec{\omega}_i|}\right)\tanh\left(\tfrac{1}{2}\beta|\vec{\omega}_i|\right) \,. \tag{12}$$

This vectorial equation is equivalent to a system of three equations for the components $\langle I_x^i\rangle$, $\langle I_y^i\rangle$, and $\langle I_z^i\rangle$ of $\langle \vec{I}_i \rangle$. If there are N spins in the sample, Eq. (12) summarizes a system of $3N$ equations which has, for every value of β, a number of solutions. Among these solutions we must select those for which all components $\langle I_x^i\rangle$, $\langle I_y^i\rangle$, and $\langle I_z^i\rangle$ are real numbers.

The next step consists of determining among all these solutions the one that is stable. We can use three different forms for the thermodynamic stability criterion. We give first these forms for systems that can be found only at positive temperatures. The stable state among many possible states of the system is as follows: at constant temperature, the state for which the free energy $F = E - TS = E - S/\beta$ is minimum (we use units for which $\hbar = k_B = 1$); at constant energy, the state for which

the entropy is maximum; at constant entropy, the state for which the energy is minimum.

When dealing with nuclear spin systems we choose the zero of energy to be that of the system at infinite temperature. Systems at positive temperature then have negative energies and systems at negative temperature have positive energies. It can be shown that in the process or preparation of the system (that is, adiabatic demagnetization from a high field) the sign of the energy and therefore also the sign of the temperature cannot change. The determination of stable structures has to be made independently for positive temperatures (i.e., negative energies) and for negative temperatures (i.e., positive energies). The former expressions for stability criterion are modified as follows. The stable structure among many possible structures whose energies have the same well-defined sign is as follows: at constant temperature the one for which $|F|$ is maximum; at constant energy the one for which S is maximum; at constant entropy the one for which $|E|$ is maximum.

The energy is given by Eq. (9). As for the entropy it is within the Weiss-field approximation equal to[21]

$$S=\sum_i \{\ln 2 - \tfrac{1}{2}[(1+p_i)\ln(1+p_i) + (1-p_i)\ln(1-p_i)]\}\,, \tag{13}$$

where p_i is the modulus of the polarization $\vec{p}_i = 2\langle \vec{I}_i \rangle$.

To summarize, the program for determining the stable structures is made of two steps: (i) Find at all temperatures all structures satisfying Eq. (12); (ii) use the stability criterion to find among these the stable ones as a function of temperature, energy, or entropy. This program cannot be fulfilled for it is in general not possible to find all solutions of Eq. (12) at arbitrary values of temperature.

The procedure that is adopted, less general than the one just outlined, is based on the following points:

(i) It is possible to find all solutions of Eq. (12) in the limiting case when all $\langle \vec{I}_i \rangle$ are vanishingly small.

(ii) We can use the stability criterion to determine the stable structure in this limiting case.

(iii) Among the structures that satisfy Eq. (12) in the limiting case, some remain solutions of these equations at all temperatures (to within a scaling of the values of p_i) whereas many do not. At an arbitrary temperature we know then but a few of all possible solutions of Eq. (12), corresponding to these "permanent" structures.

(iv) The relative stability of these permanent structures does not depend on temperature.

(v) When in the limiting case of small polarizations the stable structure is a permanent one we make the hypothesis that this structure remains stable at all temperatures with respect to *all* solutions of Eq. (12) although we only know this to be true with respect to a few of them.

(vi) When in the limiting case of small polarizations the stable structure is not a permanent one this procedure yields no answer as to the ordered structure.

In the rest of this section we analyze these various points and then use this analysis to predict the ordered structures in a simple cubic lattice.

A. Generalities on the solutions of local Weiss-field equations

The limit when all $|\langle \vec{I}_i \rangle|$ are infinitely small corresponds by definition to the critical temperature for the ordered structure. The Weiss-frequency magnitudes $|\vec{\omega}_i|$ are also small in this limit and we can replace in Eq. (12) the hyperbolic tangent by its argument:

$$\langle \vec{I}_i \rangle = -\tfrac{1}{4}\beta_c \vec{\omega}_i\,. \tag{14}$$

Since according to Eq. (10) $\vec{\omega}_i$ is a linear combination of the various spin-component average values, Eq. (14) summarizes a system of $3N$ linear homogenous equations relating the spin-component average values of the N nuclei of the sample. It is an eigenvalue problem which has $3N$ solutions, corresponding to $3N$ values of β_c, to be determined.

Equation (14) can also be written

$$\vec{\omega}_i = \lambda \langle \vec{I}_i \rangle\,, \tag{15}$$

with

$$\lambda = -4/\beta_c = -4k_B T_c/\hbar\,. \tag{16}$$

Equations (14) and (15) correspond to structures where the Weiss-field experienced by a given spin is proportional to the magnetization of that spin, with a proportionality constant identical for all spins.

We now analyze the various structures satisfying Eq. (15). According to the form (10) of $\vec{\omega}_i$, Eq. (15) corresponds to the following set of equations:

$$-\sum_j A_{ij}\langle I_x^j \rangle - \lambda \langle I_x^i \rangle = 0\,, \tag{17a}$$

$$-\sum_j A_{ij}\langle I_y^j \rangle - \lambda \langle I_y^i \rangle = 0\,, \tag{17b}$$

$$2\sum_j A_{ij}\langle I_z^j \rangle - \lambda \langle I_z^i \rangle = 0\,. \tag{17c}$$

To proceed further, we introduce the following Fourier transforms:

$$\vec{I}(\vec{k}) = N^{-1/2}\sum_i e^{i\vec{k}\cdot\vec{r}_i}\vec{I}_i\,, \tag{18}$$

$$A(\vec{k}) = \sum_i A_{ij} e^{i\vec{k}\cdot(\vec{r}_i - \vec{r}_j)} , \tag{19}$$

where $\vec{r}_i$ is the vector joining the origin (taken at a lattice site) to the location of the spin I_i, and $\vec{k}$ is one of the N vectors of the reciprocal lattice belonging to the first Brillouin zone.

Equation (19) is meaningful only insofar as the sum over i is independent of index j, a question that will be examined later on. Let us assume for the moment that this is the case. According to Eq. (19), $A(-\vec{k}) = A^*(\vec{k})$. On the other hand, since the lattice has a center of symmetry, we have $A(-\vec{k}) = A(\vec{k})$ so that all $A(\vec{k})$ are real numbers.

By an elementary and standard calculation, the system of Eqs. (17) is transformed into

$$[-A(\vec{k}) - \lambda]\langle I_x(\vec{k})\rangle = 0 , \tag{20a}$$

$$[-A(\vec{k}) - \lambda]\langle I_y(\vec{k})\rangle = 0 , \tag{20b}$$

$$[2A(\vec{k}) - \lambda]\langle I_z(\vec{k})\rangle = 0 . \tag{20c}$$

The $3N$ solutions of Eqs. (20) are of two different types: longitudinal and transverse. They are listed below.

1. Longitudinal structures

Let $\vec{k}_0$ be a given vector $\vec{k}$. Equations (20) are satisfied by the choice:

$$\begin{aligned} &\lambda = 2A(\vec{k}_0), \quad \langle I_z(\vec{k}_0)\rangle \neq 0, \quad \langle I_z(-\vec{k}_0)\rangle \neq 0 , \\ &\langle I_z(\vec{k})\rangle = 0 \quad \text{for } \vec{k} \neq \pm\vec{k}_0 , \\ &\langle I_x(\vec{k})\rangle = \langle I_y(\vec{k})\rangle = 0 \quad \text{for all vectors } \vec{k} . \end{aligned} \tag{21}$$

Inverting Eq. (18)

$$\vec{I}_i = N^{-1/2} \sum_{\vec{k}} e^{-i\vec{k}\cdot\vec{r}_i}\, \vec{I}(\vec{k}) , \tag{22}$$

we get

$$\begin{aligned} &\langle I_z^i\rangle = N^{-1/2}[e^{-i\vec{k}_0\cdot\vec{r}_i}\langle I_z(\vec{k}_0)\rangle + e^{i\vec{k}_0\cdot\vec{r}_i}\langle I_z(-\vec{k}_0)\rangle] , \\ &\langle I_x^i\rangle = \langle I_y^i\rangle = 0 . \end{aligned} \tag{23}$$

The condition $\langle I_z^i\rangle$ equals a real number is satisfied by choosing $\langle I_z(-\vec{k}_0)\rangle = \langle I_z(\vec{k}_0)\rangle^*$. This can be done in two independent ways. For instance,

$$\langle I_z(\vec{k}_0)\rangle = \langle I_z(-\vec{k}_0)\rangle = \epsilon$$

or

$$\langle I_z(\vec{k}_0)\rangle = -\langle I_z(-\vec{k}_0)\rangle = i\epsilon .$$

The value of ϵ is arbitrary and is only bound to be small.

We have then found two independent degenerate solutions for each couple of values $\pm\vec{k}_0$, except when $+\vec{k}_0$ is not distinct from $-\vec{k}_0$, in which case there is only one solution. This happens when $\vec{k}_0 = 0$ and when $\vec{k}_0$ is at the boundary of the first Brillouin zone. There are then as many independent longitudinal solutions as distinct vectors $\vec{k}$ in the first Brillouin zone, that is, N.

2. Transverse structures

For every couple of vectors $\pm\vec{k}_0$ of the first Brillouin zone there are four independent solutions of Eqs. (20). We can have

$$\begin{aligned} &\lambda = -A(\vec{k}_0), \quad \langle I_x(\vec{k}_0)\rangle \neq 0, \quad \langle I_x(-\vec{k}_0)\rangle \neq 0 , \\ &\langle I_x(\vec{k})\rangle = 0 \qquad \text{for } \vec{k} \neq \pm\vec{k}_0 , \\ &\langle I_y(\vec{k})\rangle = \langle I_z(\vec{k})\rangle = 0 \quad \text{for all } \vec{k} ; \end{aligned} \tag{24}$$

from which, for individual spins,

$$\begin{aligned} &\langle I_x^i\rangle = N^{-1/2}[e^{-i\vec{k}_0\cdot\vec{r}_i}\langle I_x(\vec{k}_0)\rangle + e^{i\vec{k}_0\cdot\vec{r}_i}\langle I_x(-\vec{k}_0)\rangle] , \\ &\langle I_y^i\rangle = \langle I_z^I\rangle = 0 . \end{aligned} \tag{25}$$

$\langle I_x^i\rangle$ is real if $\langle I_x(\vec{k}_0)\rangle = \langle I_x(-\vec{k}_0)\rangle^*$. This can be achieved in two independent ways, which yields two independent solutions.

We can also have

$$\begin{aligned} &\lambda = -A(\vec{k}_0), \quad \langle I_y(\vec{k}_0)\rangle \neq 0, \quad \langle I_y(-\vec{k}_0)\rangle \neq 0 , \\ &\langle I_y(\vec{k})\rangle = 0 \qquad \text{for } \vec{k} \neq \pm\vec{k}_0 , \\ &\langle I_x(\vec{k})\rangle = \langle I_z(\vec{k})\rangle = 0 \quad \text{for all } \vec{k} ; \end{aligned} \tag{26}$$

from which

$$\begin{aligned} \langle I_y^i\rangle = N^{-1/2}[&e^{-i\vec{k}_0\cdot\vec{r}_i}\langle I_y(\vec{k}_0)\rangle \\ &+ e^{i\vec{k}_0\cdot\vec{r}_i}\langle I_y(-\vec{k}_0)\rangle] . \end{aligned} \tag{27}$$

Again, $\langle I_y^i\rangle$ is real if $\langle I_y(\vec{k}_0)\rangle = \langle I_y(-\vec{k}_0)\rangle^*$, which can be achieved in two independent ways and yields two independent solutions.

These four solutions are degenerate, so that their linear combinations are also solutions of Eqs. (20).

Taking into account all N vectors $\vec{k}$ of the first Brillouin zone we have $2N$-independent transverse solutions, which together with the N longitudinal solutions solve the problem of finding all solutions of Eqs. (20). Each different value of λ corresponds to a different critical temperature, according to Eq. (16).

The great simplicity of the solutions is a direct consequence of the use of a truncated dipole-dipole interaction. When the full dipole-dipole interaction is used, that is, for the study of magnetic ordering in actual zero field, the z component of the Weiss field $\vec{H}_i$, for instance, depends on the various $\langle I_z^j\rangle$, but also on the various $\langle I_x^j\rangle$ and $\langle I_y^j\rangle$. The theory leads, in place of Eqs. (20), to a set of three equations for each vector $\vec{k}$, of the form

$$a\langle I_x(\vec{k})\rangle + b\langle I_y(\vec{k})\rangle + c\langle I_z(\vec{k})\rangle = 0 .$$

This system has to be diagonalized by a rotation

a priori different for each value of $\vec{k}$. Although possible, the calculations are much more complicated than in the present case.

One should remember that all these structures have been determined as viewed from the rotating frame. Longitudinal structures look the same in the laboratory frame as in the rotating frame. As for transverse structures they correspond, when viewed from the laboratory frame, to spin orientations that are rotating at the Larmor frequency around the dc field H_0. Ordering in these structures merely implies fixed *relative* orientations of the various spins.

For comparing the solutions found in the limiting case of vanishingly small polarizations one can use a power expansion of the entropy (13) with respect to p_i, which yields

$$S \simeq N\ln 2 - \frac{1}{2}\sum_i p_i^2 \ . \tag{28}$$

The energy is, according to Eqs. (9) and (15), equal to

$$E = \frac{1}{2}\sum_i \lambda \left|\langle \vec{I}_i \rangle\right|^2 = \tfrac{1}{8}\lambda \sum_i p_i^2 \ , \tag{29}$$

or else

$$E = \tfrac{1}{4}\lambda(N\ln 2 - S) \ . \tag{29'}$$

According to the third form of the stability criterion the stable structures at constant entropy in this limiting case are as follows: at positive temperature the structure for which λ is minimum ($\lambda < 0$); at negative temperature the structure for which λ is maximum ($\lambda > 0$). It is easily found that the two other forms of stability criterion predict the same stable structures.

The determination of stable structures goes as follows. We first determine the vector $\vec{k}_1$ that makes $A(\vec{k}_1)$ minimum and the vector $\vec{k}_2$ that makes $A(\vec{k}_2)$ maximum.

The structure that is stable at positive temperature is either longitudinal with $\vec{k}_0 = \vec{k}_1$, the corresponding λ being $\lambda_1 = 2A(\vec{k}_1)$; or transverse with $\vec{k}_0 = \vec{k}_2$, the corresponding λ being $\lambda_2 = -A(\vec{k}_2)$, depending on which λ is smaller.

The structure that is stable at negative temperature is either longitudinal with $\vec{k}_0 = \vec{k}_2$, the corresponding λ being $\lambda_2' = 2A(\vec{k}_2)$; or transverse with $\vec{k}_0 = \vec{k}_1$, the corresponding λ being $\lambda_1' = -A(\vec{k}_1)$, depending on which λ is larger.

Our next task is to find among all $3N$ structures determined above those that are "permanent." A structure is defined by the relative values of polarizations $\vec{p}_i$. It is said to be permanent if a change of temperature effects all magnitudes p_i by the same factor, that is, according to Eqs. (10), if the relation (15) remains valid. The permanent structures are then those that satisfy both Eqs. (12) and (15), i.e.,

$$\tanh(\tfrac{1}{2}\beta\left|\vec{\omega}_i\right|) = -\lambda\left|\vec{\omega}_i\right| \ . \tag{30}$$

This is possible only if $|\vec{\omega}_i|$ is independent of the subscript i, which implies that

$$\left|\langle \vec{I}_i \rangle\right| = \left|\lambda^{-1}\vec{\omega}_i\right| = a \ , \tag{31}$$

where a is a constant depending on β.

General solutions of Eq. (30), found by direct inspection, are the following.

Longitudinal permanent structures. They are of three different kinds.

(i) $\vec{k}_0 = 0$, $\langle I_z(0)\rangle \neq 0$. This corresponds to $\langle I_z^i \rangle$ = const, that is, to a ferromagnetic structure.

(ii) $\vec{k}_0$ is at the boundary of the Brillouin zone. We have then $e^{-i\vec{k}_0\cdot\vec{r}_i} = e^{i\vec{k}_0\cdot\vec{r}_i} = \pm 1$. If we choose $\langle I_z(\vec{k}_0)\rangle = \langle I_z(-\vec{k}_0)\rangle = \frac{1}{2}aN^{1/2}$, $\langle I_z^i \rangle$ is according to Eq. (23) alternatively equal to $+a$ and $-a$ in successive planes perpendicular to $\vec{k}_0$. This corresponds to antiferromagnetic structures consisting of planes of magnetization alternatively parallel and antiparallel to the dc field H_0.

(iii) $2\vec{k}_0$ is at the boundary of the Brillouin zone. $e^{-i\vec{k}_0\cdot\vec{r}_i} = (-i)^n$ in the nth plane from the origin perpendicular to $\vec{k}_0$. By choosing

$$\langle I_z(\vec{k}_0)\rangle = (\tfrac{1}{2}a)N^{1/2}(1+i)$$

and

$$\langle I_z(-\vec{k}_0)\rangle = (\tfrac{1}{2}a)N^{1/2}(1-i) \ ,$$

we get from Eq. (23)

$$\langle I_z^i \rangle = +a \quad \text{for the planes } 0, 1, 4, 5, 8, 9, \text{ etc.} \ ,$$

$$\langle I_z^i \rangle = -a \quad \text{for the planes } 2, 3, 6, 7, 10, 11, \text{ etc.}$$

This corresponds to an antiferromagnetic structure consisting of pairs of adjacent planes alternatively parallel and antiparallel to H_0.

Transverse permanent structures. For every couple of vectors $\pm\vec{k}_0$ it is possible to find a permanent structure that is a linear combination of solutions (25) and (26). If we choose

$$\langle I_x(\vec{k}_0)\rangle = \langle I_x(-\vec{k}_0)\rangle = (\tfrac{1}{2}a)N^{1/2} \ ,$$

$$\langle I_y(\vec{k}_0)\rangle = -\langle I_y(-\vec{k}_0)\rangle = i(\tfrac{1}{2}a)N^{1/2} \ ,$$

we get, according to Eq. (23),

$$\langle I_x^i \rangle = a\cos(\vec{k}_0\cdot\vec{r}_i) \quad \text{and} \quad \langle I_y^i \rangle = a\sin(\vec{k}_0\cdot\vec{r}_i) \ .$$

This corresponds to a helical structure where, along the direction $\vec{k}_0$, the magnetization rotates in a plane perpendicular to H_0.

There may exist other permanent structures depending on the particular values of the $A(\vec{k})$ in specific cases.

As permanent structures correspond to

$$p_i = 2\left|\langle \vec{I}_i \rangle\right| = p = \text{const} \ ,$$

the entropy and the energy take the forms

$$S = N\{\ln 2 - \tfrac{1}{2}[(1+p)\ln(1+p) + (1-p)\ln(1-p)]\}\ , \quad (32)$$

$$E = \tfrac{1}{8}N\lambda p^2\ . \quad (33)$$

Different permanent structures have equal entropies when they have equal spin polarizations p. According to the third form of stability criterion and Eq. (33) the most stable structure among them is that of minimum λ at positive temperature and that of maximum λ at negative temperature. This criterion of relative stability is exactly the same as in the limiting case of small polarization, as stated earlier.

B. Stable structures in a cubic lattice

The Fourier transforms of the dipole-dipole interactions have been computed by Cohen and Keffer[22] for various cubic lattices. They have tabulated, for a series of discrete values of $\vec{k}$ regularly distributed in the Brillouin zone, the following quantities:

$$S_3(\vec{k}) = \rho^{-1}{\sum_l}' |\vec{r}_l|^{-3} e^{i\vec{k}\cdot\vec{r}_l}\ ,$$

$$S_5^{ij}(\vec{k}) = \rho^{-1}{\sum_l}' r_l^i r_l^j |\vec{r}_l|^{-5} e^{i\vec{k}\cdot\vec{r}_l}\ ,$$

where $i, j = X, Y, Z$, the primed sums are taken over all lattice vectors $\vec{r}_l$ except $\vec{r}_l = 0$, and ρ is the number of lattice points per unit volume. The axes X, Y, Z are aligned with the fourfold axes of the cubic system. Let α, β, and γ be the cosines of the direction z of the field H_0 with respect to X, Y, and Z. The dipolar sum $A(\vec{k})$ is equal to

$$A(\vec{k}) = n\frac{\gamma^2\hbar}{2a^3}\{S_3(\vec{k}) - 3[\alpha^2 S_5^{XX}(\vec{k}) + \beta^2 S_5^{YY}(\vec{k}) + \gamma^2 S_5^{ZZ}(\vec{k}) + 2\alpha\beta S_5^{XY}(\vec{k}) + 2\beta\gamma S_5^{YZ}(\vec{k}) + 2\alpha\gamma S_5^{XZ}(\vec{k})]\}\ , \quad (34)$$

where a is the lattice parameter, and n is the number of spins per unit cell.

The following general remarks can be made in connection with these dipolar sums.

(i) For $\vec{k} = 0$ the sum $A(0) = \sum_i' A_{ij}$ is well defined, i.e., independent of subscript j provided the shape of the sample is an ellipsoid.[23] Important values of this sum are the following:

Spherical sample,

$$A(0) = 0\ ;$$

Infinity flat disk perpendicular to z,

$$A(0) = \frac{8\pi}{3}\frac{\gamma^2\hbar}{2a^3}n\ ;$$

Infinity long needle parallel to z,

$$A(0) = -\frac{4\pi}{3}\frac{\gamma^2\hbar}{2a^3}n\ .$$

(ii) When $|\vec{k}|^{-1}$ is much smaller than the sample dimensions the sum $A(\vec{k})$ is well defined. Let, for instance, R be the radius of a spherical sample. The condition is $|\vec{k}|R \gg 1$. When $|\vec{k}|^{-1}$ is large compared with the lattice parameter a, while still much smaller than R, the lattice sum has a very simple value:

$$A(\vec{k}) = \frac{\gamma^2\hbar n}{2a^3}\frac{4\pi}{3}(3\cos^2\theta_k - 1)\ , \quad (35)$$

where θ_k is the angle between the vector $\vec{k}$ and the direction z.

(iii) When $|\vec{k}|^{-1}$ becomes comparable with the sample dimensions, that is, in a sphere when $|\vec{k}|R \sim 1$, $A(\vec{k})$ is not well defined since the sum (19) depends on the subscript j. This is due to the long range of dipole-dipole interactions. $A(\vec{k})$ has been computed in this range with the spin j at the center of a sphere. The result is

$$A(\vec{k}) = \frac{\gamma^2\hbar n}{2a^3}\frac{4\pi}{3}(3\cos^2\theta_k - 1)\left(1 - \frac{3j_1(kR)}{kR}\right)\ ,$$

with $k = |\vec{k}|$, and j_1 is the Bessel function of order 1. It varies from 0 when $kR = 0$ to the value (35) when $kR \gg 1$. Its maximum value is about 10% larger than (35).

This unpleasant behavior of Fourier transforms is limited to values of $\vec{k}$ that constitute a very small fraction of the first Brillouin zone. We will assume that we can ignore the vectors $\vec{k}$ of this pathological domain unless they play a particular role. More explicitly, if for a particular orientation of the field H_0, the extrema values of $A(\vec{k})$ correspond to small k values, that is,

$$A(\vec{k})_{\max} = \frac{8\pi}{3}\frac{\gamma^2\hbar n}{2a^3}$$

or

$$A(\vec{k})_{\min} = -\frac{4\pi}{3}\frac{\gamma^2\hbar n}{2a^3}\ ,$$

the present mathematical technique may not be suited to predicting the ordering that will occur. These cases will in the present article be left explicitly aside. They will be treated in a future publication.

For bcc and fcc lattices the extrema values of $A(\vec{k})$ correspond actually to small k values and these lattices will not be studied.

In a simple cubic lattice, theory predicts the occurrence of three different antiferromagnetic structures: two at positive temperatures and one at negative temperature. They are the following, at some typical orientations of the magnetic field H_0.

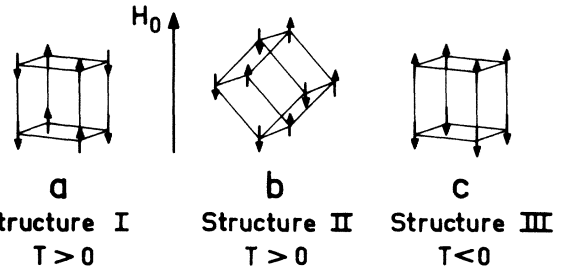

FIG. 1. Predicted antiferromagnetic structures in a simple cubic system of spins $\frac{1}{2}$ subjected to truncated dipole-dipole interactions.

1. Positive temperature

Structure I, $\vec{H}_0 \| [001]$:

$$\vec{k}_I = (\pi/a, \pi/a, 0) ,$$

$$A(\vec{k}_I) = -5.352\ \gamma^2\hbar/2a^3 , \quad \lambda_I = 2A(\vec{k}_I) , \tag{36}$$

$$T_c = -\hbar\lambda_I/4k_B = 3.4\times10^{-7}\ \text{K} . \tag{36'}$$

It is a two-sublattice antiferromagnetic structure where successive planes perpendicular to [110] have magnetizations alternatively parallel and antiparallel to [001], the direction of the dc field.

Structure II, $\vec{H}_0 \| [110]$:

$$\vec{k}_{II} = (0, 0, \pi/a) ,$$

$$A(\vec{k}_{II}) = -4.843\ \gamma^2\hbar/2a^3 , \quad \lambda_{II} = 2A(\vec{k}_{II}) , \tag{37}$$

$$T_c = 3.06\times10^{-7}\ \text{K} . \tag{37'}$$

Successive planes perpendicular to [001] have magnetizations alternatively parallel and antiparallel to [110].

2. Negative temperature

Structure III, $\vec{H}_0 \| [001]$:

$$\vec{k}_{III} = \vec{k}_{II} = (0, 0, \pi/a) ,$$

$$A(\vec{k}_{II}) = 9.687\ \gamma^2\hbar/2a^3 , \quad \lambda_{III} = 2A(\vec{k}_{II}) , \tag{38}$$

$$T_c = -6.13\times10^{-7}\ \text{K} . \tag{38'}$$

Successive planes perpendicular to [001] have magnetizations alternatively parallel and antiparallel to [001].

The structure I is known in the literature as the magnetic structure C, and structures II and III are known as structures A.[24] These structures are shown on Fig. 1.

The domain of stability of these structures is determined by the variation of the $A(\vec{k})$'s with the orientation of magnetic field $\vec{H}_0$.

For both $\vec{k}_I = (\pi/a, \pi/a, 0)$ and $\vec{k}_{II} = (0, 0, \pi/a)$ one has

$$S_5^{XY} = S_5^{YZ} = S_Z^{ZX} = 0 ,$$

$$S_5^{XX} = S_5^{YY} = \tfrac{1}{2}(S_3 - S_5^{ZZ}) ,$$

from which, according to Eq. (34),

$$A(\vec{k}_I) = -5.352\ \frac{\gamma^2\hbar}{2a^3}\ \frac{3\cos^2\theta_Z - 1}{2} ,$$

$$A(\vec{k}_{II}) = 9.687\ \frac{\gamma^2\hbar}{2a^3}\ \frac{3\cos^2\theta_Z - 1}{2} ,$$

where θ_Z is the angle between $\vec{H}_0$ and direction [001].

We will disregard the anomalous behavior of Fourier transforms for $kR \sim 1$. Then as a rough condition of stability of antiferromagnetic structures with respect to structures pertaining to small k values we have

$$A(\vec{k}) < -\frac{4\pi}{3}\ \frac{\gamma^2\hbar}{2a^3} \simeq -4.19\ \frac{\gamma^2\hbar}{2a^3} \quad \text{at } T>0 ,$$

$$A(\vec{k}) > \frac{8\pi}{3}\ \frac{\gamma^2\hbar}{2a^3} \simeq 8.38\ \frac{\gamma^2\hbar}{2a^3} \quad \text{at } T<0 .$$

It can be shown that no other structures (corresponding to different k values) interfere in this stability problem. The maps of stable structures with respect to dc-field orientation are pictured in Fig. 2 for $\frac{1}{8}$ of the entire sphere. The domains IV correspond to $A(\vec{k})$ maximum and minimum for small k values.

The boundaries correspond to the following angles:

Along AB, $\theta_Z \simeq 22^\circ$;

At C, $\theta_Z \simeq 15^\circ$;

Along BD, $\theta_X \simeq 78^\circ$;

Along L, $\theta_Z \simeq 17.5^\circ$.

The same stable antiferromagnetic structures are predicted in a crystal such as LiF. Its structure is of the NaCl type, i.e., each atomic species forms an fcc lattice. If we disregard the difference between nuclear species, we have a simple cubic lattice of nuclear magnetic spins in which is

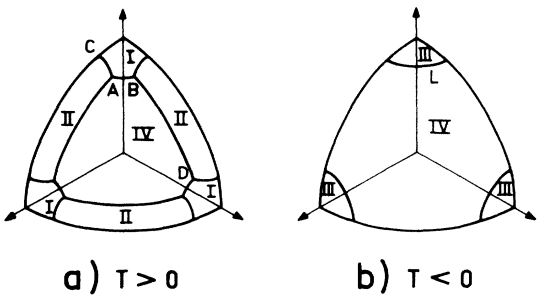

FIG. 2. Map of stable structures in a cubic system of spins $\frac{1}{2}$ with truncated dipole-dipole interactions as a function of orientation of magnetic field with respect to crystalline axes. Structures I–III are those of Fig. 1. Structures corresponding to areas IV are not analyzed.

predicted the onset at low temperature of the structures depicted above. Each sublattice of the antiferromagnetic structures would contain spins of both species. The extension to the case of several spin species of the method of the local Weiss field will not be developed here.

III. WEISS-FIELD AND HIGH-TEMPERATURE APPROXIMATION TO THE PROPERTIES OF ANTIFERROMAGNETIC STRUCTURES

We analyze now several properties of the antiferromagnetic structures, derived in Sec. II, as a function of field and entropy, within the Weiss-field approximation. It will prove, however, that this approximation is often untenable and that more elaborate treatments are required. In this article we will restrict ourselves to a very rough correction to the Weiss-field approximation based on the high-temperature approximation to spin-temperature theory. We give only the results of this high-temperature correction to the Weiss-field theory. The method for performing the high-temperature expansion of physical quantities will be published elsewhere. The analysis is mostly devoted to those properties that are amenable to measurement by NMR techniques.

Let A and B be the sublattices whose magnetizations are opposite in zero field and at low temperature. At various fields and temperatures all spins of a given sublattice have the same polarization and experience the same Weiss field. Let us call $\vec{p}_A$ and $\vec{p}_B$ the polarization vectors of each spin of sublattice A and B, respectively, and $\vec{\omega}_A^T$ and $\vec{\omega}_B^T$ the frequencies corresponding to the fields they experience. These vectors are related through

$$\vec{p}_A = -(\vec{\omega}_A^T/|\vec{\omega}_A^T|)\tanh(\tfrac{1}{2}\beta|\vec{\omega}_A^T|) , \tag{39}$$

$$\vec{p}_B = -(\vec{\omega}_B^T/|\vec{\omega}_B^T|)\tanh(\tfrac{1}{2}\beta|\vec{\omega}_B^T|) . \tag{39'}$$

The components of the frequencies are

$$\begin{aligned} \omega_{Ax}^T &= \omega_1 - \tfrac{1}{2}(qp_x^A + rp_x^B) , \\ \omega_{Ay}^T &= -\tfrac{1}{2}(qp_y^A + rp_y^B) , \\ \omega_{Az}^T &= \Delta + qp_z^A + rp_z^B ; \end{aligned} \tag{40}$$

$$\begin{aligned} \omega_{Bx}^T &= \omega_1 - \tfrac{1}{2}(qp_x^B + rp_x^A) , \\ \omega_{By}^T &= -\tfrac{1}{2}(qp_y^B + rp_y^A) , \\ \omega_{Bz}^T &= \Delta + qp_z^B + rp_z^A) , \end{aligned} \tag{40'}$$

where q and r are constants that depend on the shape of the sample and are computed below. These equations are consequences of Eqs. (10), (11), and (15). Let us consider the special case when $\vec{p}_A = \vec{p}_B$ and they are aligned along z. We have then

$$\omega_{Az}^T = \omega_{Bz}^T = \Delta + (q + r)p_z^A \tag{41}$$

or else, according to Eqs. (15) and (20),

$$\omega_{Az}^T = \Delta + A(0)p_z^A ; \tag{42}$$

from which

$$q + r = A(0) . \tag{43}$$

If, on the other hand, $\vec{p}_A = -\vec{p}_B$ along z, we have

$$\omega_{Az}^T = \Delta + (q - r)p_z^A = \Delta + A(\vec{k}_0)p_z^A , \tag{44}$$

where $\vec{k}_0$ is the vector $\vec{k}$ pertaining to the antiferromagnetic structure; from which

$$q - r = A(\vec{k}_0) , \tag{45}$$

that is,

$$\begin{aligned} q &= \tfrac{1}{2}[A(0) + A(\vec{k}_0)] , \\ r &= \tfrac{1}{2}[A(0) - A(\vec{k}_0)] . \end{aligned} \tag{46}$$

In the particular case of a spherical sample we have $A(0) = 0$ and

$$q = -r = \tfrac{1}{2}A(\vec{k}_0) . \tag{47}$$

A. Sublattice magnetization in zero field

The sublattice magnetization is the most fundamental property of an antiferromagnet. Its value can be reached in principle by neutron diffraction and by antiferromagnetic resonance.

The system contains $\frac{1}{2}N$ spins of polarization $|\vec{p}_A| = p_A$ and $\frac{1}{2}N$ spins of polarization p_B. Its entropy is, according to Eq. (13), equal to

$$S = \tfrac{1}{2}N[s(p_A) + s(p_B)] , \tag{48}$$

where $s(p)$ is the entropy per spin of polarization p in the Weiss-field approximation. In zero field we have $\vec{p}_A = -\vec{p}_B$, i.e., $|\vec{p}_A| = |\vec{p}_B| = p_A$, that is,

$$S = Ns(p_A) . \tag{48'}$$

The state of the system has been reached by adiabatic demagnetization of a paramagnetic state with all spins parallel and with equal polarizations $\vec{p}_i$.

Writing that the initial entropy

$$S_i = Ns(p_i) \tag{49}$$

is equal to the final one (48'), we get

$$p_A = p_i . \tag{50}$$

The paradoxical and obviously wrong result is that, however small the initial polarization, the system becomes antiferromagnetic upon adiabatic demagnetization. This severe deficiency of the Weiss-field approximation arises from its complete neglect of the entropy associated with short-range order. In the high-temperature approximation to spin-temperature theory[12] it is apparent that the energy and the entropy associated with the local field H_L' correspond to short-range order. Since the Weiss-field approximation knows no local field

other than the Weiss-field itself, it predicts that whatever the initial temperature in high field, adiabatic demagnetization will decrease it below the critical temperature.

It is known from other domains of magnetism that the Weiss-field value for the critical temperature T_c is not too bad an approximation to its actual value. We can attempt to get a rough approximation of the transition entropy as follows. We take for granted the Weiss-field values of T_c [Eqs. (36′), (37′), and (38′)] and we use the high-temperature approximation to spin-temperature theory to find which initial polarizations yield these temperatures after demagnetization. According to this theory, the relationship between initial and final inverse temperatures, when performing an adiabatic demagnetization from a high initial field to zero, is

$$\beta_f/\beta_i = \omega_0/D, \tag{51}$$

where ω_0 is the initial Larmor frequency and D is the local frequency, defined by

$$D^2 = \mathrm{Tr}(\mathcal{H}_D'^2)/\mathrm{Tr}(I_z^2)\ . \tag{52}$$

Since in high field and at high temperature, the polarization of a spin $\frac{1}{2}$ is equal to

$$p = -\tfrac{1}{2}\beta_i\omega_0\ ,$$

adiabatic demagnetization yields an inverse temperature equal to β_c if the initial polarization is, in absolute value,

$$p_i = p_0 = \tfrac{1}{2}D|\beta_c| = D/|A(\vec{k}_0)|\ . \tag{53}$$

Selected values of D in a simple cubic lattice are the following:

$H_0 \| [100]$, $D = 3.16\ \gamma^2\hbar/2a^3$;

$H_0 \| [110]$, $D = 1.96\ \gamma^2\hbar/2a^3$.

Figures for the three antiferromagnetic structures are the following:

Structure I, $\vec{H}_0 \| [100]$, $T > 0$:

$$p_0 = 0.59\ , \tag{54}$$

Structure II, $\vec{H}_0 \| [110]$, $T > 0$:

$$p_0 = 0.405\ , \tag{54′}$$

Structure III, $\vec{H}_0 \| [100]$, $T < 0$:

$$p_0 = 0.326\ . \tag{54″}$$

However approximate, these values are indicative of the amount of initial polarization required to see an effect after adiabatic demagnetization. This approximation will be used in various forms in the following.

B. Transverse susceptibility in zero field

In zero effective field the sublattice polarizations, aligned along z, are opposite, so that the net magnetization of the system is zero. If a small rf field H_1, which in the rotating frame is seen as a static field, is applied perpendicular to z, the sublattice polarizations tilt by a small angle θ so as to be aligned with the total field they experience. One has to first order in θ

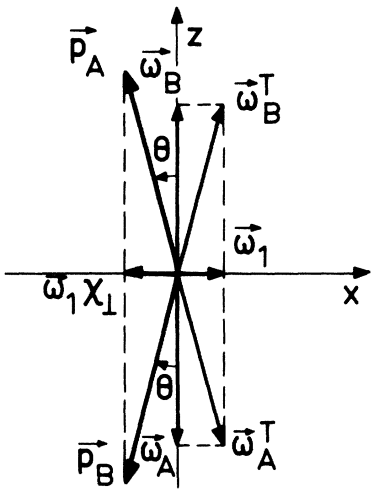

FIG. 3. Sublattice polarizations and fields for an antiferromagnet in the presence of a small transverse field. The figure corresponds to the case of a positive temperature.

$$p_{Az} = p\ ,\quad p_{Ax} = \theta p\ ,\quad p_{Ay} = 0\ , \tag{55}$$

$$p_{Bz} = -p\ ,\quad p_{Bx} = \theta p\ ,\quad p_{By} = 0\ ; \tag{56}$$

$$\begin{aligned} &\omega_{Az}^T = A(\vec{k}_0)p\ ,\quad \omega_{Ax}^T = \omega_1 - \tfrac{1}{2}A(0)\theta p\ ,\quad \omega_{Ay}^T = 0\ ,\\ &\omega_{Az}^T = -A(\vec{k}_0)p\ ,\quad \omega_{Ax}^T = \omega_1 - \tfrac{1}{2}A(0)\theta p\ ,\quad \omega_{Ay}^T = 0\ . \end{aligned} \tag{57}$$

This situation is depicted in Fig. 3. From the condition

$$\frac{p_{Ax}}{p_{Az}} = \theta = \frac{\omega_{Ax}^T}{\omega_{Az}^T} = \frac{\omega_1 - \frac{1}{2}A(0)\theta p}{A(\vec{k}_0)p}\ ,$$

we get

$$\theta = \omega_1/\{p[A(\vec{k}_0) + \tfrac{1}{2}A(0)]\}\ .$$

If we define the transverse susceptibility as

$$\chi_\perp = \frac{1}{N}\sum_i p_x^i \Big/ \omega_1\ , \tag{58}$$

we get

$$\chi_\perp = 1/[A(\vec{k}_0) + \tfrac{1}{2}A(0)]\ . \tag{59}$$

This susceptibility is *independent* of sublattice polarization in the antiferromagnetic state. This property is the first that has been predicted for antiferromagnets.[25] It has been observed to hold approximately for all antiferromagnetic systems of electronic spins.

Comparison of this behavior with that predicted

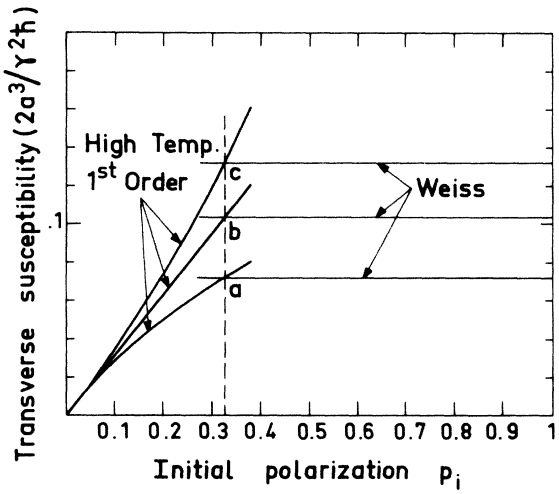

FIG. 4. Transverse susceptibility in zero field as a function of initial polarization, with $\vec{H}_0 \| [100]$ and at negative temperature, according to both the Weiss-field and the high-temperature approximations. (a) Infinitely flat disk perpendicular to H_0; (b) spherical sample; (c) infinitely long needle parallel to H_0.

at low initial polarization by spin-temperature theory offers another way of estimating the transition entropy. We suppose that we are in a paramagnetic state, so that $\vec{p}_A = \vec{p}_B = \vec{p}$ and $\vec{\omega}_A^T = \vec{\omega}_B^T = \vec{\omega}^T$. In the high-temperature approximation to spin-temperature theory we have $p_\alpha \propto \beta\omega_\alpha$ $(\alpha = x, y, z)$. Then if we start the adiabatic demagnetization with initial polarization p_i we get according to Eq. (51)

$$p_x = p_i \omega_x^T / D; \tag{60}$$

from which, according to Eqs. (40) and (43),

$$p_x = p_i[\omega_1 - \tfrac{1}{2}A(0)p_x]/D$$

or else

$$\chi_{\perp\,\mathrm{para}} = p_x/\omega_1 = p_i/[D + \tfrac{1}{2}A(0)p_i]\,. \tag{61}$$

It is equal to the value (59) in the antiferromagnetic state when the initial polarization value $|p_i|$ is equal to

$$p_0 = D/[A(\vec{k}_0)]\,.$$

This is identical with Eq. (53) and yields the same values of p_0 as Eqs. (54)–(54″).

This value of p_0 is independent of the value of $A(0)$, that is, independent of the sample shape provided it is an ellipsoid. It reflects the fact that the demagnetizating field $-\frac{1}{2}A(0)p_x$ affects in the same way the transverse susceptibility in the paramagnetic and in the antiferromagnetic state.

Figure 4 shows the variation of $\chi_\perp$ with initial polarization predicted by Eqs. (59) and (61) for structure III ($\vec{H}_0 \| [100]$ and $T<0$) for three different sample shapes: sphere, infinitely flat disk perpendicular to $\vec{H}_0$, and infinitely long needle parallel to $\vec{H}_0$.

In order to estimate the importance of nonlinear effects in spin temperature in the paramagnetic state while approaching the transition, we have computed the variation of $\chi_\perp$ with initial polarization to third order with respect to inverse temperature. This variation is shown on Fig. 5 for $H_0 \| [100]$ in a spherical sample.

On the same figure are plotted the experimental values of $\chi_\perp$ observed for ^{19}F spins in a spherical sample of CaF_2. The polarization scale was determined in these experiments by comparison of absorption signal areas with that of a thermal equilibrium signal at 4.2 K. Its accuracy is of the order of 10%. The ordinates were adjusted so as to fit the value of $\chi_\perp$ in the plateau to the theoretical value [Eq. (59)]. The over-all agreement between experiment and theory is satisfactory. The striking prediction of the theory, namely, the occurrence of a plateau in the variation of $\chi_\perp$ versus initial polarization, has also been confirmed, although only qualitatively, for $H_0 \| [100]$ and $T>0$ (corresponding to the theoretical prediction of structure I), and for $H_0 \| [110]$ and $T>0$ (corresponding to the theoretical prediction of structure II). The "turnover" initial polarizations correspond grossly to those predicted. A detailed description of these experiments together with new results will be published later.

C. Longitudinal susceptibility in zero field

Let us start in zero field with polarizations along z and $p_z^A = -p_z^B = p$, and let β be the inverse temperature corresponding to these values. We then introduce adiabatically a small field $-\Delta/\gamma$

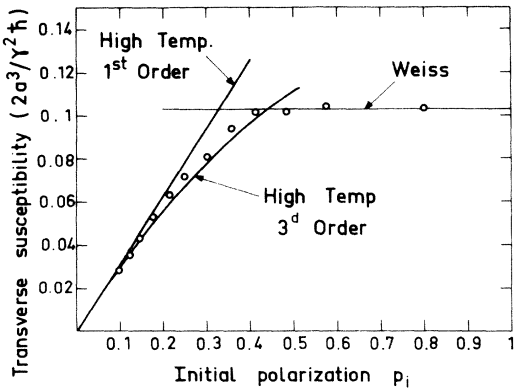

FIG. 5. Transverse susceptibility in zero field as a function of initial polarization for a spherical sample, with $\vec{H}_0 \| [100]$ and at negative temperature, according to Weiss-field, first-order high-temperature, and third-order high-temperature approximations, together with experimental results for CaF_2.

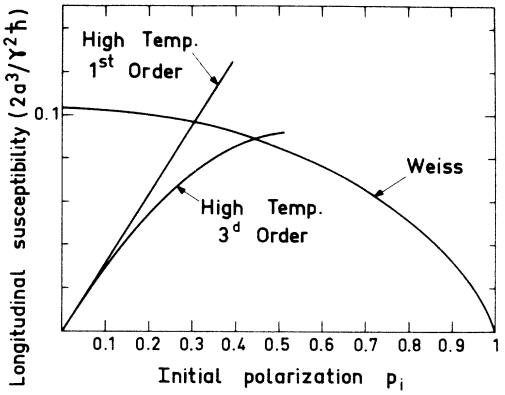

FIG. 6. Longitudinal susceptibility in zero field as a function of initial polarization for a spherical sample, with $\vec{H}_0 \| [100]$ and at negative temperature, according to Weiss-field, first-order high-temperature, and third-order high-temperature approximations.

along z and look for the total longitudinal magnetization, which is proportional to Δ. The magnetization is proportional to the isentropic longitudinal susceptibility which, as we show now, is in the present case equal to the isothermal susceptibility. Let $d\beta$ be the variation of temperature corresponding to the isentropic introduction of the field Δ. The total longitudinal magnetization is

$$M_z(\Delta, \beta + d\beta) = M_z(0, \beta) + \frac{\partial M_z(0,\beta)}{\partial \omega_z}\Delta + \frac{\partial M_z(0,\beta)}{\partial \beta} d\beta \ ,$$

while

$$dS = \frac{\partial S(0,\beta)}{\partial \omega_z}\Delta + \frac{\partial S(0,\beta)}{\partial \beta} d\beta = 0 \ .$$

Since in zero field the magnetization vanishes we have $M_z(0,\beta) = \partial M_z(0,\beta)/\partial\beta = 0$ and $M_z(\Delta, \beta + d\beta)$ does not depend on $d\beta$ to first order, which proves the statement.

In zero field the polarizations are along z and are equal to $p_z^A = -p_z^B = p$. In the field $-\Delta/\gamma$ they are equal to $p_z^A = p + \epsilon$ and $p_z^B = -p + \epsilon'$. Equations (39) and (40) yield, to first order in Δ, ϵ, and ϵ',

$$\epsilon = \epsilon' = -\tfrac{1}{2}\beta\Delta(1-p^2)/[1 + \tfrac{1}{2}\beta A(0)(1-p^2)] \ . \quad (62)$$

We define the longitudinal susceptibility as

$$\chi_{\parallel} = \frac{1}{N}\sum_i p_z^i / \Delta \ ,$$

and we get

$$\chi_{\parallel} = \epsilon/\Delta = -\tfrac{1}{2}\beta(1-p^2)/[1 + \tfrac{1}{2}\beta A(0)(1-p^2)]$$

$$= (1-p^2)\ln\left(\frac{1+p}{1-p}\right)\Big/ \left[2pA(\vec{k}_0) - A(0)(1-p^2)\ln\left(\frac{1+p}{1-p}\right)\right], \quad (63)$$

where we have used

$$-\tfrac{1}{2}\beta A(\vec{k}_0)p = \tanh^{-1}(p) = \tfrac{1}{2}\ln\left(\frac{1+p}{1-p}\right) \ .$$

In the paramagnetic case, a combination of Weiss-field and high-temperature approximations for spin-temperature theory yields for $p_z^A = p_z^B = p_z$

$$p_z = p_i[\Delta + A(0)p_z]/D \ ,$$

from which

$$\chi_{\parallel\,\text{para}} = p_i/[D - A(0)p_i] \ . \quad (64)$$

Figure 6 is a plot of $\chi_{\parallel}$ versus initial polarization according to Eqs. (63) and (64) for structure III in a spherical sample. On this figure is also plotted the variation of $\chi_{\parallel}$ in the paramagnetic phase according to third-order expansion in β, the calculation of which is not given here.

The qualitative feature of Eq. (63), namely, that in the antiferromagnetic state $\chi_{\parallel}$ decreases when the sublattice polarizations increase, is also one of the early predictions on antiferromagnetism that has been well verified in electronic spin systems. Together with the constancy of $\chi_{\perp}$ it is very characteristic of antiferromagnets. This feature has been experimentally verified by measuring $\chi_{\parallel}$ not as a function of entropy, but as a function of dipolar energy,[26] by a procedure that will not be described here. The results are shown on Fig. 7, together with the Weiss-field theoretical prediction in the antiferromagnetic state and first- and third-order high-temperature expansions in the paramagnetic state. The Weiss-field value of the dipolar energy in the antiferromagnetic state is, according to Eqs. (29) and (36)–(38) given by

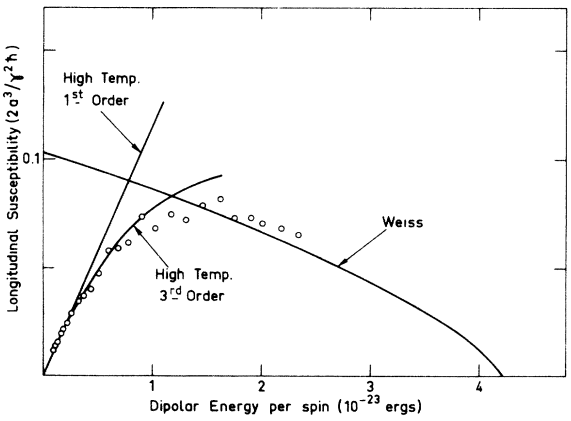

FIG. 7. Longitudinal susceptibility in zero field as a function of energy for a spherical sample of CaF_2, with $\vec{H}_0 \| [100]$ and at negative temperature, according to Weiss-field, and first-order high-temperature and third-order high-temperature approximations, together with experimental results.

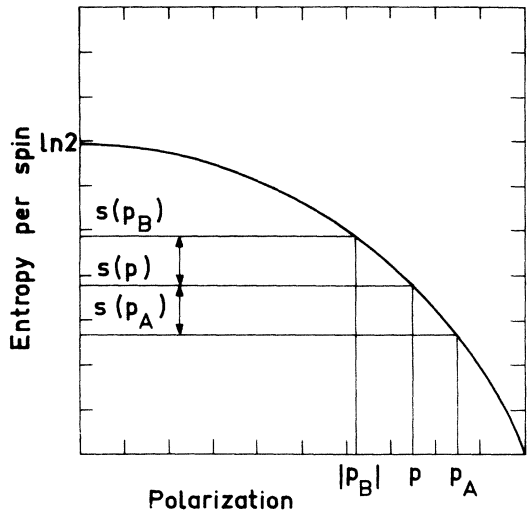

FIG. 8. Selection of a couple of values of sublattice polarizations p_A and $|p_B|$ corresponding within the Weiss-field approximation to the same entropy as the initial polarization p.

$$E_d/N = \tfrac{1}{4}A(\vec{k}_0)p^2 .$$

In the paramagnetic state, the first-order high-temperature approximation to spin-temperature theory[12] yields the value

$$E_d/N = \tfrac{1}{2}p_i D .$$

There is an over-all semiquantitative agreement between the variation of $\chi_{\parallel}$ and that predicted by the above approximate theories.

D. Sublattice polarizations, transition field, and dispersion signal during a fast passage

The fast passage, i.e., the adiabatic demagnetization followed by remagnetization, takes place at constant entropy. All properties of the antiferromagnet during a fast passage, that is, for nonzero values of Δ, are calculated from Eqs. (39), (39′), (40), (40′), and (48). We will describe but a few of these properties without giving the proofs. We will consider for simplicity the case of a spherical sample, so that $A(0) = 0$. We will limit ourselves to initial polarizations $p \lesssim 0.65$, the reason being that with initial polarizations above this value the phenomena are complicated by the occurrence, in an entropy-dependent range of nonzero effective fields, of a more complex structure whose description is postponed to a later publication.

1. Sublattice polarizations

Within the Weiss-field approximation, the sublattice polarizations are determined most simply as follows. Let p be the initial polarization. If in a field Δ/γ the polarization of sublattice A, along z, is equal to $p_z^A = p_A$, the value of $|p_z^B| = p_B$ is, according to Eq. (48), obtained from

$$s(p_A) + s(p_B) = 2s(p) , \tag{65}$$

as shown on Fig. 8. The sign of p_z^B is left undetermined.

Given values of p_z^A and p_z^B which satisfy Eq. (65) we look for values of Δ and β that satisfy Eqs. (39) and (39′), and (40) and (40′). A straightforward calculation yields

$$\Delta = \tfrac{1}{2}A(\vec{k}_0)(p_z^A - p_z^B)(u_A + u_B)/(u_A - u_B) , \tag{66}$$

where we use the notation

$$u_A = \tanh^{-1}(p_A) \quad \text{and} \quad u_B = \tanh^{-1}(p_B) .$$

The value of β can then be calculated if desired from one of Eqs. (39) and (39′).

As an example, Fig. 9 shows the variation of p_z^A and p_z^B as a function of effective field for an initial polarization $p = 0.4$. The field values correspond to CaF_2 with $\vec{H}_0 \| [100]$.

2. Transition field

It can be shown from the Weiss-field equations that when

$$2p \tanh^{-1}(p) \leq 1 ,$$

which corresponds to initial polarizations $p \leq 0.647$, the transition from paramagnetism to antiferromagnetism is of second order and takes place at the field for which $p_z^A - p_z^B \to 0$. A straightforward but tedious calculation yields for the critical field

$$\Delta_c = \tfrac{1}{2}A(\vec{k}_0)(1 - p^2) \ln\left(\frac{1+p}{1-p}\right) , \tag{67}$$

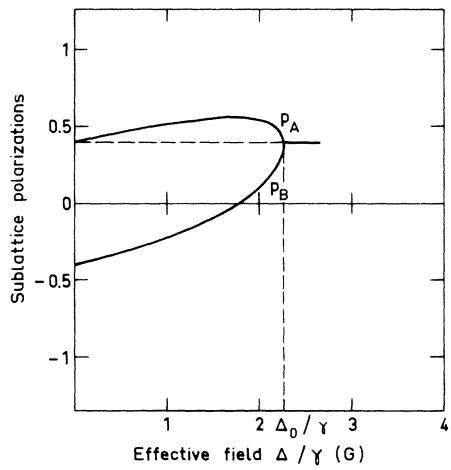

FIG. 9. Sublattice polarizations as a function of effective longitudinal field. The entropy corresponds to an initial polarization $p_i = 0.4$. Figures correspond to structure III ($\vec{H}_0 \| [100]$ and $T < 0$) in a spherical sample of CaF_2.

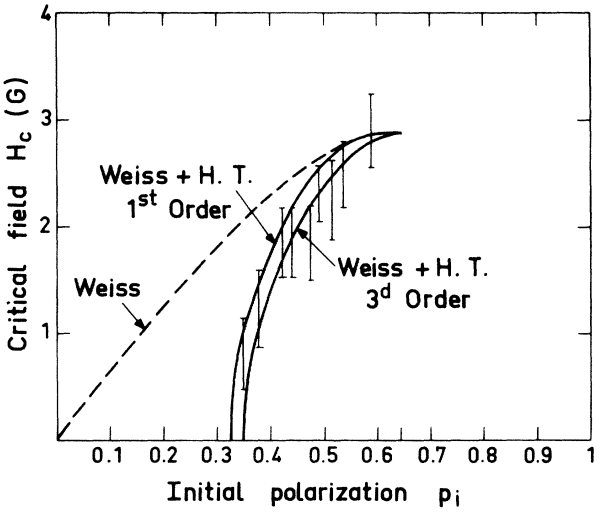

FIG. 10. Critical field as a function of initial polarization in a spherical sample of CaF_2 with structure III ($\vec{H}_0 \| [100]$, $T<0$) using Weiss-field, Weiss-field plus first-order high-temperature, and Weiss-field plus third-order high-temperature approximations. Comparison with experimental results.

and for the critical inverse temperature

$$\beta_c = -[\tfrac{1}{2}A(\vec{k}_0)(1-p^2)]^{-1} . \tag{68}$$

The variation of $H_c = \Delta_c/\gamma$ as a function of initial polarization p is plotted in Fig. 10. The figures correspond to structure III ($\vec{H}_0 \| [100]$, $T<0$) for ^{19}F spins in CaF_2.

The inadequacy of the Weiss-field approximation for accounting for the entropy is here again apparent in the unacceptable prediction that the critical field vanishes only at zero initial polarization. In an attempt to improve this result we can use the same approximation as before. Namely, we compute β_c as a function of Δ_c according to Eqs. (67) and (68). Then we use a high-temperature expansion to compute the entropy corresponding to those values of β and Δ, and finally we determine the initial polarization that corresponds to this entropy. The result, critical field as a function of initial polarization, is also plotted in Fig. 10 for first-order and third-order approximations to the entropy. This calculation corresponds to second-order transitions, when at the transition the system is paramagnetic. The "critical" initial polarizations obtained by this procedure, 0.32 and 0.345, for first-order and third-order approximations, respectively, are close to those obtained before. The formula $S = S(\beta, \Delta)$ and its derivation will be given in a forthcoming paper.

Approximate values of transition fields have been derived from the shape of the fast-passage signals described in Sec. III D3. These values are plotted on Fig. 10. However approximate, they fit reasonably the predictions of the combined Weiss-field plus high-temperature approximation.

3. *Dispersion signal*

In the presence of the rf field driving the fast passage the total spin polarization u along ω_1 is calculated by first-order perturbation. The magnitudes of the polarizations are those calculated in Sec. III D2 and these polarizations are tilted by a small angle so as to make them parallel to the total field experienced by the spins.

In the high-field paramagnetic phase we have $\vec{p}_A = \vec{p}_B = \vec{p}$, and

$$\omega_1/p_x = \Delta/p_z \simeq \Delta/p ,$$

from which

$$u = \frac{1}{N}\sum_i p_x^i = p\omega_1/\Delta \tag{69}$$

and the dispersion signal is hyperbolic. In the low-field antiferromagnetic phase a straightforward calculation yields for a spherical sample

$$\frac{u}{\omega_1} = \frac{\Delta(p_z^A + p_z^B) + \frac{1}{2}A(\vec{k}_0)[4p_z^A p_z^B - (p_z^A)^2 - (p_z^B)^2]}{2\Delta^2 + \frac{1}{2}\Delta A(\vec{k}_0)(p_z^A + p_z^B) - \frac{3}{4}A(\vec{k}_0)^2(p_z^A - p_z^B)^2} . \tag{70}$$

The variation predicted by Eqs. (69) and (70) is plotted in Fig. 11, the lower part for $p = 0.59$. The figures correspond to structure III in a spherical sample of CaF_2. In the upper part of this figure are shown experimental fast-passage signals ob-

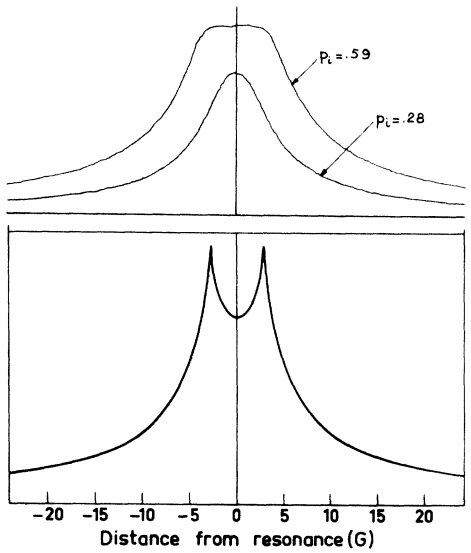

FIG. 11. Fast-passage dispersion signal in CaF_2 with $T<0$ and $\vec{H}_0 \| [100]$. Top: experimental signals with initial polarizations $p_i = 0.59$ and 0.28. Bottom: signal predicted by Weiss-field approximation for $p_i = 0.59$.

served in a spherical sample of CaF_2 at negative temperature and with $\vec{H}_0 \| [100]$ for two values of initial polarization: 59 and 28%. The singularity predicted by the Weiss-field approximation at the passage from paramagnetism to antiferromagnetism is to a large extent smeared out in the experimental signal with $p_i = 0.59$. It reduces to a plateau that begins at an effective field comparable to the theoretical transition field. This plateau is observed in the range of initial polarizations for which the transverse susceptibility in zero field $\chi_\perp$ is constant. Such a shape departs markedly from the usual shape of fast-passage signals at high temperature, as exemplified by the fast-passage signal corresponding to $p_i = 0.28$.

IV. CONCLUSION

This article consists essentially of two parts. In the first part we have described the general principles underlying the production and study of magnetic ordering in nuclear spin systems. The problem of producing magnetic ordering is essentially that of cooling the nuclear spins to sufficiently low temperatures. It is solved by a two-step process: dynamic polarization in a high field followed by nuclear adiabatic demagnetization either in the laboratory frame or in the rotating frame. A consequence of this procedure is that the temperature is not the most accessible experimental parameter. We have listed with few details a number of measurements that can be made and the kind of information they yield on the properties of the ordered state. Most of these measurements use the technique of nuclear magnetic resonance and as such they depart markedly from those used to investigate electronic spin systems.

The second part of the article makes use of a particular approximation method, the Weiss-field approximation, to derive the main properties of the ordered states: the nature of the ordered structures and the variation with entropy of some of the physical quantities amenable to measurement. This investigation is limited to systems consisting of a simple cubic array of one nuclear species of spins $\frac{1}{2}$ subjected to truncated dipole-dipole interactions. The same methods can of course be used to study more complex situations: a nontruncated spin-spin Hamiltonian in actual zero field, more complex crystalline structures, spins higher than $\frac{1}{2}$, the existence of scalar as well as dipolar interactions between spins and the presence of several spin species. The limited ambition of using the simplest possible approximation to get a qualitative picture of the phenomena proves insufficient insofar as, because of the poor value of entropy yielded by the Weiss-field method, the latter gives a completely erroneous prediction for the transition from paramagnetism to antiferromagnetism. An attempt is made to amend these faulty predictions by combining the Weiss-field approximation with the high-temperature approximation to spin-temperature theory. The most severe criticism that can be made to this method is that the results it yields are inconsistent from the point of view of thermodynamics. This point will be analyzed in detail in a future article where we will develop a closely related approximation in a consistent way.

Nuclear-magnetic-resonance measurements give no direct proof of the existence of antiferromagnetism, contrary to neutron diffraction. The purpose of the NMR investigation must be to measure as many quantities as possible, to calculate them by as good theories as possible and to hope for overall agreement. The experimental results obtained so far exhibit semiquantitative agreement with the makeshift theory given above as regards parallel and perpendicular susceptibilities and transition fields, and qualitative agreement as regards the shape of fast-passage signals. In any case they provide strong support to the existence of nuclear-dipolar antiferromagnetism.

The occurrence of a magnetic phase transition under such unusual conditions as effective interactions in a rotating frame and negative absolute temperature illustrates the quality of nuclear spin systems as model systems for thermodynamics. These studies give furthermore a physical meaning to temperatures in the microdegree range that would, for other systems, be hardly distinguishable from absolute zero.

ACKNOWLEDGMENTS

We acknowledge the contribution of R. Pick, who introduced us to the methods of the determination of ordered structures. J.-F. Jacquinot and S. Cox, "second generation" investigators of nuclear magnetic ordering, have been of great help for clarifying and decanting our ideas. This work has benefited from many discussions with J. Winter.

[1] A. Abragam, C. R. Acad. Sci. (Paris) 251, 225 (1960).
[2] A. Abragam, C. R. Acad. Sci. (Paris) 254, 1267 (1962).
[3] M. Goldman, in *Magnetic Resonance and Radiofrequency Spectroscopy*, edited by P. Averbuch (North-Holland, Amsterdam, 1969), p. 157.
[4] M. Chapellier, M. Goldman, Vu Hoang Chau, and A. Abragam, C. R. Acad. Sci. (Paris) 268, 1530 (1969).
[5] M. Chapellier, M. Goldman, Vu Hoang Chau, and A. Abragam, J. Appl. Phys. 41, 849 (1970).
[6] M. Chapellier, in *Proceedings of the Twelfth International Conference on Low Temperature Physics*, edited by Eizo Kanda (Keigaku, Tokyo, 1971), p. 637.

[7]Vu Hoang Chau, thesis, C.N.R.S. No. 708 (Orsay, 1970) (unpublished).
[8]M. Goldman, Pure Appl. Chem. 32, 137 (1972).
[9]S. Cox, in Conference on Low Temperature Physics, Moscow, 1973 (unpublished).
[10]M. Goldman, in *Pulsed Nuclear Magnetic Resonance and Spin Dynamics in Solids*, edited by J. W. Hennel (Institute of Nuclear Physics, Cracow, Poland, 1973), p. 91.
[11]J.-F. Jacquinot, W. T. Wenckebach, M. Chapellier, M. Goldman, and A. Abragam, C. R. Acad. Sci. (Paris) B 278, 93 (1974).
[12]See, for instance, M. Goldman, *Spin Temperature and NMR in Solids* (Clarendon, Oxford, England, 1970).
[13]W. K. Rhim, A. Pines, and J. S. Waugh, Phys. Rev. B 3, 684 (1971).
[14]A. Abragam and W. G. Proctor, C.R. Acad. Sci. (Paris) 246, 2253 (1958).
[15]A. Abragam, *The Principles of Nuclear Magnetism* (Clarendon, Oxford, England, 1961), Chap. III.
[16]F. Keffer and C. Kittel, Phys. Rev. 85, 329 (1952).
[17]I. I. Gurevich and L. V. Tarasov, *Low Energy Neutron Physics* (North-Holland, Amsterdam, 1968).
[18]A. Abragam, G. L. Bacchella, H. Glättli, P. Meriel, J. Piesvaux, and M. Pinot, C.R. Acad. Sci. (Paris) 274, 423 (1972).
[19]A. Abragam, G. L. Bacchella, C. Long, P. Meriel, J. Piesvaux, and M. Pinot, Phys. Rev. Lett. 28, 805 (1972).
[20]J. Villain, J. Phys. Chem. Solids 11, 303 (1959).
[21]W. Bragg and E. Williams, Proc. R. Soc. A 145, 609 (1934).
[22]M. H. Cohen and F. Keffer, Phys. Rev. 99, 1128 (1955).
[23]L. D. Landau and E. M. Lifschitz, *Electrodynamics of Continuous Media* (Pergamon, New York, 1960).
[24]See, for example, A. Herpin, *Théorie du Magnétisme* (Presses Universitaires de France, Paris, 1968), p. 589.
[25]L. Néel, Ann. Phys. (Paris) 17, 5 (1932).
[26]J.-F. Jacquinot, M. Chapellier, and M. Goldman (unpublished).